

## Flow Characteristics over a Missile at Higher Angle of Attacks using Experiments and Simulation

M. Ramakrishna<sup>a</sup>, M. Syedhaleem<sup>b</sup>, C. Divya<sup>a</sup> and A. Gurunathan<sup>a</sup>

<sup>a</sup>Tagore Engg. College, Chennai, Tamilnadu, India

<sup>b</sup>Bharath Institute of Higher Education and Research, Chennai, Tamilnadu, India

Corresponding Author, Email: [syedhaleem.aero@bharathuniv.ac.in](mailto:syedhaleem.aero@bharathuniv.ac.in)

### ABSTRACT:

*The need to determine forces and moments acting on bodies of revolution at high angles of attack originally arose in connection with airships. In general missile aerodynamics is dominated with vertical and separated flows. The advent of highly manoeuvrable missile design concepts has required a major effort in understanding the problem of slender bodies of revolution at high angles of attack. An extensive experimental investigation was conducted to determine the aerodynamic forces and moments. The aerodynamic data are needed to establish the structural and control system requirements. Tests were conducted on a smooth missile model with several interchangeable nose parts in a wind tunnel at subsonic level at high angle of attack. The yaw moments and side forces are determined using force measuring systems by which maximum induced side force was found. Using oil flow visualization technique, vortex shedding location and vortex strength were traced at various angles of attack. Computational analysis was carried out for the cone, elliptical and ogive nose shapes. It is then compared with the experimental results to know where the least flow separation occurs and proper reasons for the side forces.*

### KEYWORDS:

*Missile; Subsonic flow; Angle of attack; Wind tunnel; Computational fluid dynamics*

### CITATION:

M. Ramakrishna, M. Syedhaleem, C. Divya and A. Gurunathan. 2018. Flow Characteristics Over a Missile at Higher Angle of Attacks using Experiments and Simulation, *Int. J. Vehicle Structures & Systems*, 10(1), 10-13. doi:10.4273/ijvss.10.1.03.

## 1. Introduction

The flight envelopes of modern aircraft and missiles include very high angle of attacks. Hence, extensive knowledge of the aerodynamics of wing and body combinations over a large range of angles of attacks is required. Deng et al [1-2] used manual setting of mini-perturbations to obtain the repeatable and determinate asymmetric vortex flow at the nose of a missile model and correlated the multi-vortices structure to the section side force distribution. Bak et al [3] investigated the aerodynamic characteristics of a missile with grid fin both experimentally and numerically. The investigation was carried out for an angle of attack range of  $-15^\circ$  to  $+15^\circ$ . They have concluded that the grid fin configuration produces greater normal force coefficient than a planar fin.

Lee et al [4] studied the effect of an elliptic tip and its eccentricity on the control of side force acting on an ogive cylinder. It was concluded that the tip with larger eccentricity reduces the onset angle of attack and delays the disappearance of side force to higher angles of attack [5]. Viswanath [6] investigated the effectiveness of nose bluntness and axial nose blowing to control the side force arising due to vortex asymmetry. Several reviews of the development of the current knowledge of body aerodynamics have been presented by Earl et al [8]. The

following four regimes occur over an angle of attack range of bodies from  $0^\circ$  to  $90^\circ$ :

- Vortex free flow at angles up to about  $15^\circ$ .
- Symmetric vortex flow at moderate angles of about  $15$  to  $30^\circ$ .
- Steady asymmetric vortex flow at higher angles of about  $30^\circ$  to  $60^\circ$ .
- Unsteady, wake like vortex flow at very high angles of about  $60^\circ$ .

The most spectacular flow phenomenon is the occurrence of a large asymmetric flow separation, with a large accompanying side force.

In this work, tests were conducted on a smooth missile model with several interchangeable nose parts in a wind tunnel at subsonic level at high angle of attack. Using oil flow visualization technique, vortex shedding location and vortex strength were traced at various angles of attack. Computational analysis was carried out for the cone, elliptical and ogive nose shapes. It is then compared with the experimental results to know where the least flow separation occurs and proper reasons for the side forces.

## 2. Experimental methodology

The Conical nose, Elliptic nose and Ogive nose of missile are designed using standard formulae and have been shown in Figs. 1 to 3 respectively. All the

dimensions except the nose are the same for all three configurations. Table 1 lists the key dimensions for the missile design. The calibration of the tunnel is ensured such that the total pressure remains as constant throughout the test section to continue further experiments in the same tunnel [7]. A pitot rake with 26 ports is kept in the test section such that the ports are parallel to the flow direction. These are connected to the water columns of a multi tube manometer from which the total pressure is measured. The model with cruciform fins and l/d ratio of 12.5 has been designed with a wind tunnel blockage ratio of 5%. Flow visualization enables us to visualize the flow patterns. Oil flow visualization is used for this test. Droplets of oil are placed on the model prior to wind tunnel run for visualization.



Fig. 1: 2D model of conical nose missile

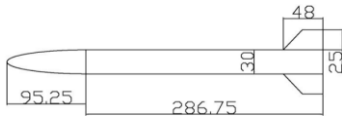


Fig. 2: 2D model of elliptical nose missile

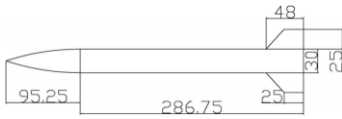


Fig. 3: 2D model of ogive nose missile

Table 1: Missile dimensions for cruciform fin type

Description	Value	Description	Value
Length of missile	382mm	Ct	23.812mm
l/d	12.7	Cr	47.6mm
l/dn	3.2	Aspect ratio	2
Nose length	95.25mm	b/2	23.81mm

### 3. Results and discussions

The oil flow visualizations from the wind tunnel tests for conical, elliptical and ogive nose configuration have been shown in Figs. 4, 6, and 8 respectively. Computational fluid dynamics analysis is carried out using ANSYS software for the higher angle of attack being 30° for validation of the test results. Figs. 5, 7 and 9 show the static pressure fringe plot from the ANSYS simulation for the conical, elliptical and ogive nose configuration respectively. At angle of attack 0° shows that there is no occurrence of vortex formation throughout the entire missile. At angle of attack 10°, there is no formation of vortex near the nose for the conical case whereas there is a slight vortex formation for the elliptical case and a symmetric vortex formation for the ogive case. At angle of attack 20°, symmetric vortex is formed over the entire body for the conical case, whereas, the vortex has started to shed in the elliptical case and the symmetric vortex prevails in the case of the ogive body. At angle of attach 30°, the vortex has developed further downstream for the conical case, whereas the symmetric vortex is developed and spread

throughout the body for the other cases. At angle of attack 40°, for both the conical case and the ogive case, the asymmetric vortex has started to appear while in the elliptical case, the vortex still remains symmetric. At angle of attack 50°, asymmetric vortex is noted further downstream for the conical and the ogive case and asymmetric flow has started to appear for the elliptical case. At angle of attack 60°, development of asymmetric vortex further downstream is seen for all the cases. The conical nose as the nose is very sharp the formation of vortex flow takes place at lower angle of attack than the other types of nose. Asymmetric vortex formation takes places at much faster rate for the conical nose than the other two types of nose.

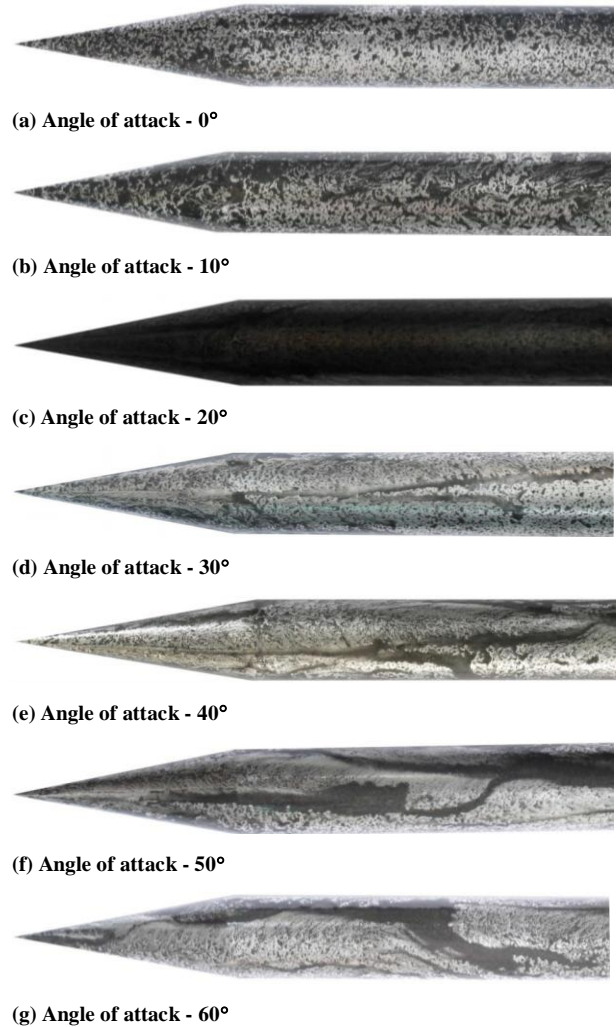


Fig. 4: Oil flow visualization for conical nose for Re = 25,000

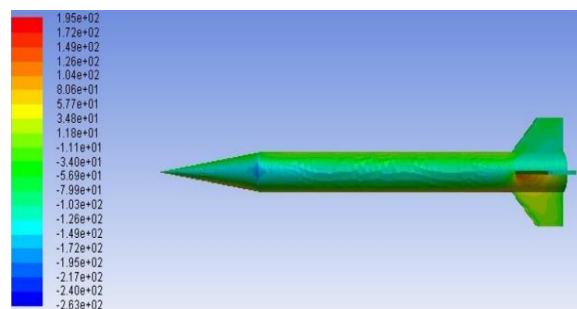


Fig. 5: static pressure (MPa) contours for conical nose, Re = 25,000, Angle of attack = 30°

For elliptical nose, the vortex formation is symmetric up to 40° angle of attack. The asymmetric vortex starts to shed from the body at 50° angle of attack. This asymmetric vortex shedding is very high and sudden at 60° angle of attack.

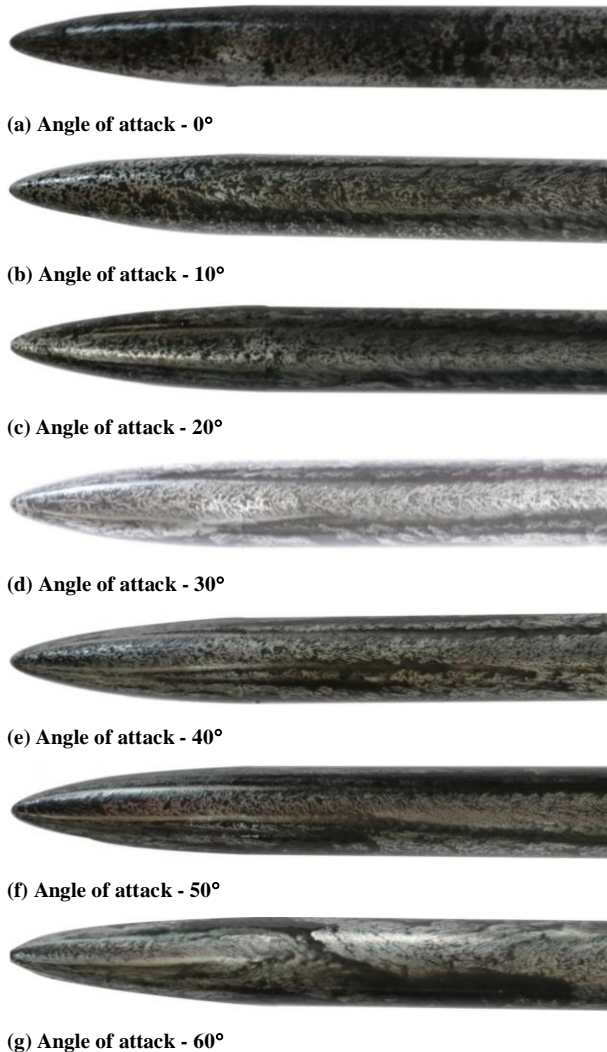


Fig. 6: Oil flow visualization for elliptical nose for Re = 25,000

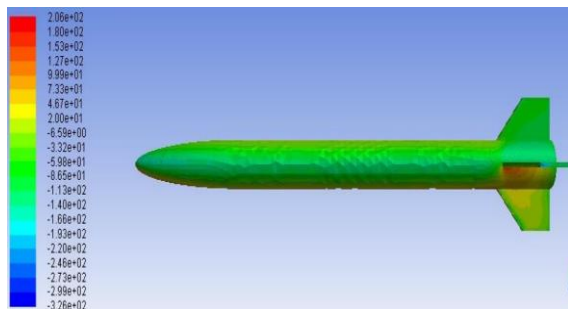


Fig. 7: Static pressure contour for elliptical nose, Re = 25,000, Angle of attack = 30°

For the ogive nose, the flow is symmetric up to 30° angle of attack. The flow becomes asymmetric as the angle of attack approaches 40°. At 60° angle of attack, the asymmetric vortex formation is clearly visible in the oil flow visualization method.

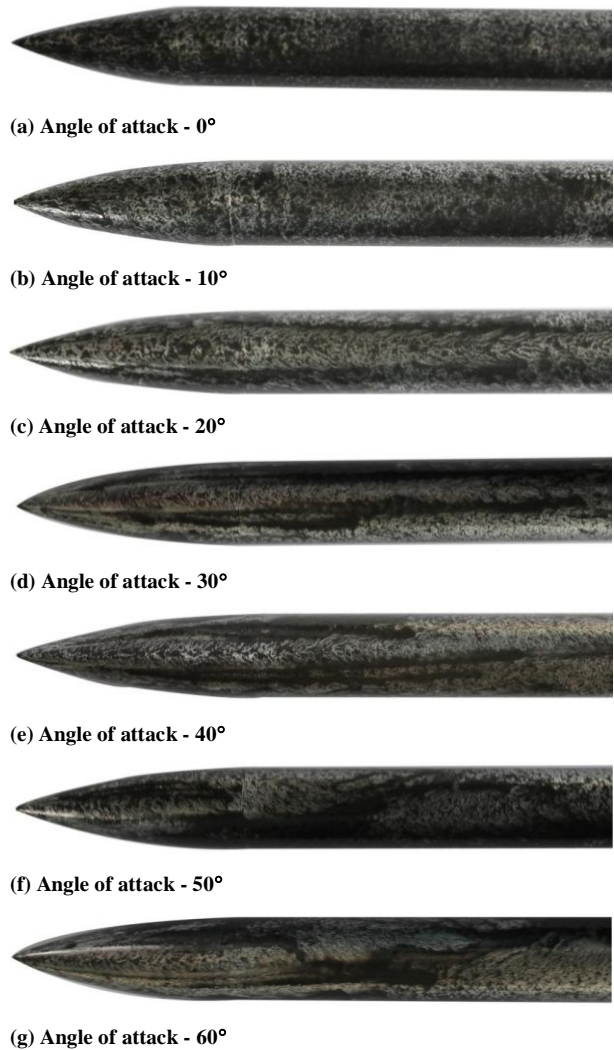


Fig. 8: Oil flow visualization for ogive nose for Re = 25,000

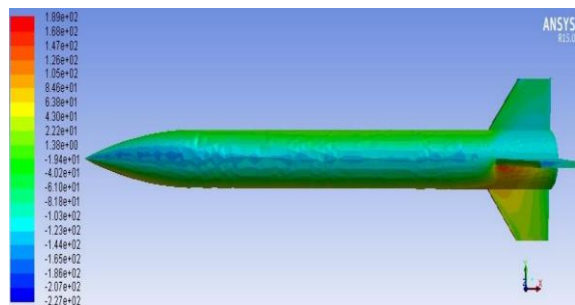


Fig. 9: Static pressure contours for ogive nose, Re = 25,000, Angle of attack = 30°

#### 4. Conclusion

An analytical study has been carried out to analyze the asymmetric flow around a slender body at different angles of attack. From the oil flow visualization and analysis, at higher angles of attack has been visualized and the basic flow physics behind the slender body aerodynamics has been studied. Thus the understanding of these asymmetric vortices is essential for predicting the aerodynamic forces during manoeuvring. From the results of oil flow and analysis it is found that elliptical and ogive is best suitable for the surface to air missile than the conical nose as they are able to delay the formation and development of asymmetric vortices which lead to high values of side force making the

control of the missile is difficult. Also, other than the side force, the normal force was also calculated and it was found that the elliptic and ogive shapes gives better aerodynamic efficiency compared to the conical nose.

#### REFERENCES:

- [1] D. Xueying and W. Gang. 2013. A physical model of asymmetric vortices flow structure in regular state over slender body at high angle of attack, *Sci. in China (Series E)*, 46(6), 561-573.
- [2] D. Xueying and W. Yankui. 2004. Asymmetric vortex flow and its active control at high angle of attack, *Acta Mechanica Sinica*, 20(6), 567-579.
- [3] K.M. Bak. 2010. Experimental investigation and computational fluid dynamics analysis of missile with grid fin in subsonic flow, *Int. J. Engg. Sci. and Tech.*, 2(11), 6214-6220.
- [4] A.S. Lee, S.C. Luo, T.T. Lim, K.B. Lua and E.K.R. Goh. 2000. Side force on an ogive cylinder: Effects of control devices, *AIAA J.*, 38(3), 385-388. <http://dx.doi.org/10.2514/2.981>
- [5] M. Gad-El-Hak and C.M. Ho. 1986. Unsteady flow around an ogive cylinder, *J. Aircraft*, 23, 520-528. <https://doi.org/10.2514/3.45338>.
- [6] P.R. Viswanath. 2008. Some aspects of vortex asymmetry and its control on slender bodies at high angles of attack, *Proc. 12<sup>th</sup> Asian Congress of Fluid Mechanics*, Daejeon, Korea.
- [7] A. Roshko. 1961. Experiments on the flow past a circular cylinder at very high Reynolds number, *J. Fluid Mechanics*, 10(3), 345-356. <https://doi.org/10.1017/S0022112061000950>.
- [8] E.R. Keener, G.T. Chapman, L. Cohen and J. Taleghani. 1977. Side force on a tangent ogive fore body with a fineness ratio of 3.5 at high angles of attack and Mach numbers from 0.1 to 0.7, *NASA TM X-3437*.